Accurate protein-peptide titration experiments by nuclear magnetic resonance using low-volume samples

Christian Kohler, Raphaël Recht, Marc Quinternet, Frédéric de Lamotte, Marc-André Delsuc, Bruno Kieffer

Metadata of the chapter that will be visualized online

Chapter Title	Accurate Protein–Peptide Titration Experiments by Nuclear Magnetic Resonance Using Low-Volume Samples	
Copyright Year	2015	
Copyright Holder	Springer Science+Business Media New York	
Author	Family Name	**Köhler**
	Particle	
	Given Name	**Christian**
	Suffix	
	Organization	Institut de Génétique et de Biologie Moléculaire et Cellulaire
	Address	1, rue Laurent Fries, BP 1014267404 Illkirch Cedex, France
Author	Family Name	**Recht**
	Particle	
	Given Name	**Raphaël**
	Suffix	
	Organization	Institut de Génétique et de Biologie Moléculaire et Cellulaire
	Address	1, rue Laurent Fries, BP 1014267404 Illkirch Cedex, France
Author	Family Name	**Quinternet**
	Particle	
	Given Name	**Marc**
	Suffix	
	Division	FR CNRS-3209 Bioingénierie Moléculaire, Cellulaire et Thérapeutique (BMCT)
	Organization	CNRS, Université de Lorraine
	Address	Biopôle, Campus Biologie Santé, CS 5018454505 Vandœuvre-lès-Nancy Cedex, France
Author	Family Name	**Lamotte**
	Particle	de
	Given Name	**Frederic**
	Suffix	
	Organization	INRA, UMR AGAP
	Address	34398 Montpellier Cedex 5, France
Author	Family Name	**Delsuc**
	Particle	
	Given Name	**Marc-André**
	Suffix	
	Organization	Institut de Génétique et de Biologie Moléculaire et Cellulaire
	Address	1, rue Laurent Fries, BP 1014267404 Illkirch Cedex, France

Corresponding Author	Family Name	**Kieffer**
	Particle	
	Given Name	**Bruno**
	Suffix	
	Organization	Institut de Génétique et de Biologie Moléculaire et Cellulaire
	Address	1, rue Laurent Fries, BP 1014267404 Illkirch Cedex, France
	Email	kieffer@igbmc.fr

Abstract	NMR spectroscopy allows measurements of very accurate values of equilibrium dissociation constants using chemical shift perturbation methods, provided that the concentrations of the binding partners are known with high precision and accuracy. The accuracy and precision of these experiments are improved if performed using individual capillary tubes, a method enabling full automation of the measurement. We provide here a protocol to set up and perform these experiments as well as a robust method to measure peptide concentrations using tryptophan as an internal standard.

Keywords (separated by '-')	Affinity measurements - Protein–peptide interactions - NMR - Equilibrium binding constants

Chapter 22

Accurate Protein–Peptide Titration Experiments by Nuclear Magnetic Resonance Using Low-Volume Samples

Christian Köhler, Raphaël Recht, Marc Quinternet, Frederic de Lamotte, Marc-André Delsuc, and Bruno Kieffer

Abstract

NMR spectroscopy allows measurements of very accurate values of equilibrium dissociation constants using chemical shift perturbation methods, provided that the concentrations of the binding partners are known with high precision and accuracy. The accuracy and precision of these experiments are improved if performed using individual capillary tubes, a method enabling full automation of the measurement. We provide here a protocol to set up and perform these experiments as well as a robust method to measure peptide concentrations using tryptophan as an internal standard.

Key words Affinity measurements, Protein–peptide interactions, NMR, Equilibrium binding constants

1 Introduction

Nuclear Magnetic Resonance (NMR) provides a powerful tool to study protein–ligand and protein–protein interactions at atomic resolution [1]. Among many other possibilities, NMR can be used to measure very accurately the equilibrium constant of the interaction, provided that its equilibrium dissociation constants (K_d) is in the range of 10 μM or above, a value that corresponds to the study of rather weak interactions. Several methods have been developed to measure protein–ligand dissociation constants, and they are usually classified in two main classes: the "ligand-observed" and the "protein-observed" methods. While "ligand-observed" methods, such as Saturation Transfer Difference (STD) or WaterLogsy share common principles with other biophysical approaches, the "protein-observed" approach is unique to NMR for its ability to deliver site-specific information [2, 3]. Thanks to these properties, NMR is now an established tool in pharmaceutical industry where it is used in drug discovery strategies, essentially at

Senta Reichelt (ed.), *Affinity Chromatography: Methods and Protocols*, Methods in Molecular Biology, vol. 1286,
DOI 10.1007/978-1-4939-2447-9_22, © Springer Science+Business Media New York 2015

the hit-to-lead step, where low to medium affinity ligands are gradually optimized into potent ligands [4]. The classical approach to study ligand–protein interactions relies on the measurement of protein chemical shift perturbations (CSP) induced by the binding of the ligand. This is generally performed using proteins that are enriched with magnetically active isotopes such as nitrogen 15 or carbon 13 and the prior knowledge of the protein resonance assignments that links a measured nucleus frequency to the corresponding molecular site. The chemical shift perturbations are then monitored using heteronuclear correlation spectra upon successive addition of increasing amounts of ligand. This approach is applicable to very large protein complexes such as the proteasome or the nucleosome, provided that appropriate labeling strategies are used such as the selective labeling of methyl groups [5]. It has been recently shown that this approach is also applicable with non-labeled protein samples thanks to the latest progress in NMR spectrometer sensitivity and the use of relaxation optimized pulse sequences such as Methyl SOFAST [6]. For proteins with molecular weights of less than 20 KDa, the common approach relies on the cost-effective production of ^{15}N labeled samples and the use of highly sensitive ^{1}H–^{15}N HSQC correlation spectra to monitor CSP. Here, we present a protocol enabling the equilibrium dissociation constants between a binding peptide and a small protein to be measured with high precision and accuracy. The method relies on the use of several low-volume samples, an approach that provides better accuracy when compared to the classical sequential titration method [7]. The protocol takes advantage of the ability to quantify precisely the amount of ligand present in the different samples as an accurate knowledge of the active concentrations of the interacting partners determines the reliability of the final result. The practical aspects of these measurements are illustrated using the interaction between the third SH3 domain of Vinexinβ and a model polyproline peptide from the N-terminal domain (NTD) of the Retinoic Acid Receptor γ (RARγ) as a prototypal case (Fig. 1). In this particular study, both accurate and precise measurements of K_d values for different peptides are needed to understand the molecular basis of the affinity modulation by the phosphorylation of the RARγ NTD [8].

2 Materials

2.1 Protein Production

The protein is obtained using heterologous expression in *E coli* according a protocol that depends on the system under study. Produce 4–5 mg of purified ^{15}N labeled protein using adapted expression and a purification protocols (*see* **Note 1**).

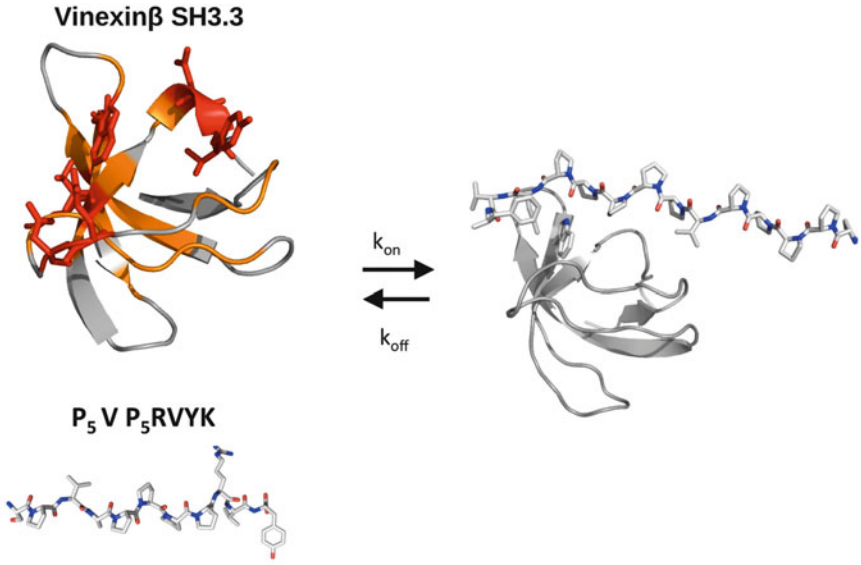

Fig. 1 The titration protocol presented here is illustrated with data originating from an interaction study between a model peptide from the proline-rich region of the RARγ NTD and the third SH3 domain of the human Vinexinβ [8]. The residues highlighted in orange and red show Chemical Shift Perturbation (CSP) of their $^{1}H–^{15}N$ correlation peaks upon addition of increasing amounts of peptide, indicating the location of the binding site on the protein surface. The CSP of *red highlighted* residues that were used to fit the equilibrium dissociation constant K_d

2.2 Peptide Synthesis

Peptides are obtained from the peptide synthesis platform at IGBMC using an ABI 443A synthesizer adapted to FMOC chemistry. Purify the crude peptide products by reverse phase high performance liquid chromatography (HPLC) before undergoing a second chromatographic purification step in a migration column containing a cluster of resin balls (stable phase). Check the purity (95 % or better) of the resulting product by examining the HPLC elution profile, and by analyzing the peptide by mass spectrometry and NMR (*see* **Note 1**).

2.3 Capillary System

Use 1.7 mm outer-diameter capillary system for NMR measurements. This system is composed of 75 mm long capillaries capped with a teflon tube which is placed into a sample holder. Use a sample volume of 50 µL, which produces a filling height of 40 mm that was tested to be sufficient. The sample holders have a standard 5 mm outer diameter upper section with a transition to a 3 mm outer diameter (60 mm long) stem. The sample holder is reusable and fits all conventional 5 mm rotors. Fill the space between the capillary and the sample holder with 50 µL of D_2O (deuterated water) for the external lock. The system was purchased from "New-Era" (Vineland, NJ, USA).

2.4 NMR Measurements

The NMR measurements should be performed using a high-field (above 600 MHz) NMR spectrometer equipped with a triple resonance cryogenic probe. Set the acquisition parameters to keep the measurement time within reasonable limits of 1–2 h per titration point. If available, use a sample changer to run the experiment unattended overnight (*see* **Note 2**).

2.5 Theoretical Aspects of K_d Measurements from NMR Frequencies

The binding of a ligand peptide (L) to a protein (P) to form a peptide–protein complex (PL) is described by the following equilibrium:

$$P + L \underset{k_{\text{off}}}{\overset{k_{\text{on}}}{\rightleftharpoons}} PL \tag{1}$$

The dissociation equilibrium constant K_d is defined as:

$$K_d = \frac{k_{\text{off}}}{k_{\text{on}}} = \frac{[P]\,[L]}{[PL]} \tag{2}$$

Where $[P]$, $[L]$ and $[PL]$ are the concentrations of the free protein, the free ligand and the complex respectively and k_{on} and k_{off} the association and dissociation rates respectively. The ability to determine the value of the dissociation constant from chemical shift measurements depends on the exchange kinetic between free and bound species, defined as:

$$k_{\text{exc}} = k_{\text{off}} + k_{\text{on}}[L] \tag{3}$$

For k_{exc} values significantly larger than the NMR frequency difference $2\pi\left(\nu_i^{\text{bound}} - \nu_i^{\text{free}}\right)$ between the bound and free states of the protein, the observed frequency, ν_i is a weighted average between the frequencies of the free and bound states:

$$\nu_i = x_1\nu_i^{\text{bound}} + (1 - x_i)\nu_i^{\text{free}} \tag{4}$$

$x_i \in [0, 1]$ is the occupancy of a given binding site i within the protein. This averaging situation occurs when k_{off} is rather fast, which corresponds to ligands of weak affinity (in the micromolar to millimolar range). Assuming that the frequency change of a given nucleus within the protein is essentially due to local perturbations, its value provides therefore a direct measurement of the occupancy of the binding site localized in its vicinity using:

$$x_i = \frac{\nu_i - \nu_i^{\text{free}}}{\nu_i^{\text{bound}} - \nu_i^{\text{free}}} \tag{5}$$

The subscript i highlights the unique ability of NMR spectroscopy to measure site-specific affinity binding constants. The value of the site-specific dissociation constant, K_d^i, is subsequently obtained using a nonlinear fit of the following equation:

$$x_i^2 - x_i\left(1 + \frac{[L]_0}{[P]_0} + \frac{K_d^i}{[P]_0}\right) + \frac{[L]_0}{[P]_0} = 0 \quad (6)$$

with: $[L_0] = [L] + [PL]$ and $[P_0] = [P] + [PL]$

$K_d{}^i$ and $\nu_i{}^{\text{bound}}$ are adjustable parameters to minimize the value of the target function:

$$f\left(K_d^i, \nu_i^{\text{bound}}\right) = \frac{1}{N}\sum_{j=1}^{N}\left(\nu_{i,j}^{\text{calc}} - \nu_{i,j}^{\text{obs}}\right)^2 \quad (7)$$

$\nu_{i,j}{}^{\text{calc}}$ is a frequency calculated for a given total concentrations of protein $[P]_{0,j}$ and ligand $[L]_{0,j}$, using equations (Eqs. 4 and 6) while $\nu_{i,j}{}^{\text{obs}}$ is the corresponding measured frequency. The subscript j identifies each single titration point from the total number of N different mixtures of protein and ligand.

The protein frequencies are usually measured using ^{15}N or ^{13}C labeled proteins and heteronuclear correlation spectra. For small proteins, such as a SH3 domain, ^{1}H–^{15}N correlation spectra provide an inexpensive and accurate way to monitor the chemical shift perturbations induced by the binding of a ligand. Both nitrogen and its bound amide proton frequencies are reported using a composite chemical shift (frequency) usually defined as:

$$\delta_{\text{comp}} = \sqrt{\delta_{^{15}\text{N}}^2 + \left(\frac{\gamma_{\text{H}}}{\gamma_{\text{N}}}\delta_{^1\text{H}}\right)^2} \quad (8)$$

3 Methods

3.1 Design of the NMR Titration Experiment

1. The feasibility of the affinity measurement by NMR will depend on the K_d value and the ability to get the protein and the peptide at concentrations that are compatible with NMR measurements. The minimal protein concentration required to acquire ^{1}H–^{15}N heteronuclear correlation spectra varies between 10 and 100 μM, depending on the available NMR spectrometer. Check with classical methods (UV, DLS, …) whether the protein of interest can be concentrated up to these values using a non-labeled protein sample.
2. Check the quality of the ^{15}N labeled sample by recording a ^{1}H–^{15}N HSQC spectrum of your stock protein solution at its highest concentration. Standard large volume NMR tubes (5 or 3 mm tubes) can be used for this purpose. Check the stability of the protein sample at the planned measurement temperature by recording a ^{1}H–^{15}N HSQC spectrum after a few days at this temperature. The appearance of a subset of sharp peaks is indicative of protein degradation (*see* **Note 3**).

3. Desalt the peptide and transfer it to the buffer used for the protein. Both steps could be done at once using a gel filtration column such as the Superdex Peptide 10/300 GL (*see* **Note 4**).
4. Since the method presented here is only applicable when the protein–peptide interaction leads to a so-called "fast exchange regime," it is important to check whether this condition holds true for the system of interest at an early stage of the study. This could be done by preparing an initial sample with approximately stoichiometric concentrations of protein and peptide and by recording a $^{1}H–^{15}N$ HSQC spectrum of this sample. Four distinct situations may be encountered:
   - The correlation map of the mixture is identical to the one obtained for the sole protein, indicative of an absence of interaction.
   - The spectrum displays broader correlation peaks and several peaks are missing. This case corresponds to more complex situations where the protein undergoes an intermediate time-scale exchange between two (peptide-bound and free) or more states, preventing K_d measurements.
   - A second set of correlation peaks is observed. This is indicative of a "slow exchange regime" corresponding to tight interactions between the protein and the peptide. No quantitative measurement of the K_d will be possible using chemical shift measurements.
   - The correlation map of the mixture contains the same number of peaks, but several of these peaks have different frequencies when compared to the peptide-free spectrum of the protein. This situation will allow the measurement of the K_d.

3.2 Measurement of Peptide and Protein Concentrations

Several factors do affect the accuracy and precision of equilibrium constant measurements by NMR, the most important one being inaccurate estimations of protein and ligand concentrations (*see* **Note 5**). While the protein concentration may be measured with reasonable accuracy using its absorption at 280 nm, this is not the case for the peptides, in particular when they lack tryptophan or tyrosine residues. It is therefore essential to ensure an accurate measurement of protein and peptide concentrations. We report hereafter a simple method that provides reasonable accuracy for peptide concentration measurements by NMR (below 10 %) (*see* **Note 6**).

1. Prepare a stock solution of tryptophan by weighting about 6 mg of L-Tryptophan (MW: 204.23 g/mol). Dissolve the powder in 5 mL of D_2O 99.9 %.

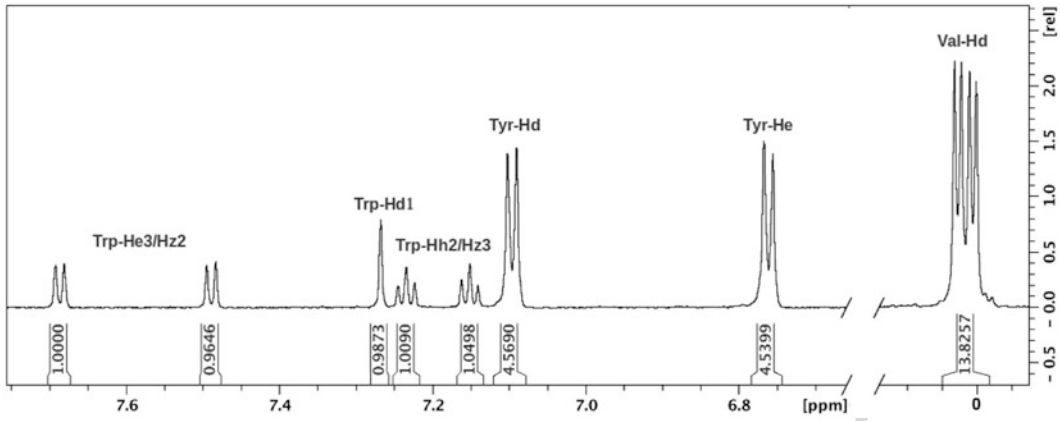

Fig. 2 1D proton spectrum of a mixture between a model peptide (sequence P_5VP_5RVYK) corresponding to the proline-rich region of the RARγ NTD and the tryptophan solution of known concentration. The amount of peptide required for this concentration measurement was 15–20 μg. The ratio between the averaged integrals of the tryptophan peaks and those of the peptide indicated that the peptide was 2.3 times more concentrated than the tryptophan. Given the concentration of the tryptophan standard, this led to concentration of 4.5 ± 0.2 mM for the peptide stock solution. The relative uncertainty on the peptide concentration using this method was 4.4 %

2. Measure the concentration of the L-Tryptophan stock solution (5–6 mM) by measuring the absorption at 280 nm (ε_{280} = 5,690 $mol^{-1} \cdot cm^{-1}$) (*see* **Note 7**).
3. Prepare a NMR sample by mixing a small volume (10–20 μL) of peptide (whose stock solutions are usually available at millimolar concentration) with (5–20 μL) of L-Tryptophan stock solution. Complete with D_2O to get a total sample volume of 150–170 μL, suitable for a 3 mm tube.
4. Record a 1D proton NMR spectrum of the sample with water pre-saturation for solvent signal suppression. Adjust the number of scans to get a reasonable signal-to-noise ratio according the sensitivity of your spectrometer. A long relaxation delay (10–15 s) should be used to account for the long T1 of the tryptophan aromatic protons (about 3 s) (Fig. 2).
5. Perform a baseline correction and integrate the signals of the tryptophan aromatic protons as well as one or few isolated resonance peaks of the peptide (we often use methyl groups resonances). Compute the ratio between the areas (normalized by the number of protons resonating at the corresponding frequency) measured for the peptide and the tryptophan to get the concentration of the peptide stock solution $[L]_0$ using:

$$[L]_0 = \frac{A_L N_w}{A_w N_L} \frac{DF_L}{DF_w} [W]_0 \quad (9)$$

Where A_L is the areas measured under one or several peaks corresponding to N_L proton resonances of the peptide. A_w and

N_w are the corresponding values obtained for the tryptophan resonances. DF_L and DF_w are the dilution factors used to prepare the sample from the peptide and the tryptophan stock solutions, respectively. $[W]_0$ is the concentration of the tryptophan stock solution determined in **step 2**.

6. Measure the protein concentration using its absorption at 280 nm.

3.3 NMR Capillaries Preparation and NMR Acquisition

1. Prior the titration experiment, the protein concentration needed to achieve a reasonable signal-to-noise (S/N) ratio on the heteronuclear $^{1}H–^{15}N$ HSQC spectra should be adjusted. On a 700 MHz equipped with a cryoprobe, a protein concentration (the SH3.3 domain of Vinexin β) of 50 to 80 μM in a 1.7 mm capillary tube provides good quality spectra. This will highly depend on the available NMR equipment as well as on the system under study. The use of NMR capillary tubes is of particular interest when titration experiments have to be performed in high salt concentrations (*see* **Note 8**). As an example, the comparison of relative sensitivity measured on SH3 samples using standard 5 mm, 3 mm tubes and capillary tubes at 700 MHz is provided in Table 1. Despite the apparent reduced signal-to-noise ratio observed for low-volume samples, the relative sensitivity (sensitivity per amount of material) is significantly increased, up to a factor of 3 with capillaries as shown in Table 1 (*see* **Note 9**).
2. Prepare the different protein–peptide mixtures in Eppendorf tubes. Adjust the sample volume according the capacity of the chosen capillaries. For 1.7 mm capillaries, the volume is adjusted to 75 μL using the protein buffer (*see* **Note 1**). Fill the capillaries using a stretched Pasteur pipette or a Hamilton syringe. Add 50 μL buffer in the capillary holder for external lock. After capping the capillaries, insert them within the capillary holder as shown in Fig. 3. As an example, we provide here a sample preparation table (Table 2) that was used to measure the

Table 1
Experimental sensitivities per amount of protein, relative to a 5 mm (550 μL) NMR tube

Sample geometry	550 μL 5 mm tube 9 % D_2O in sample	180 μL 3 mm tube 9 % D_2O in sample	50 μL capillary 9 % D_2O in sample	50 μL capillary no D_2O in sample
Ratio of protein material	1	0.33	0.09	0.1
HSQC S/N	763	569	179	241
Relative sensitivity	**1**	**2.26**	**2.61**	**3.16**

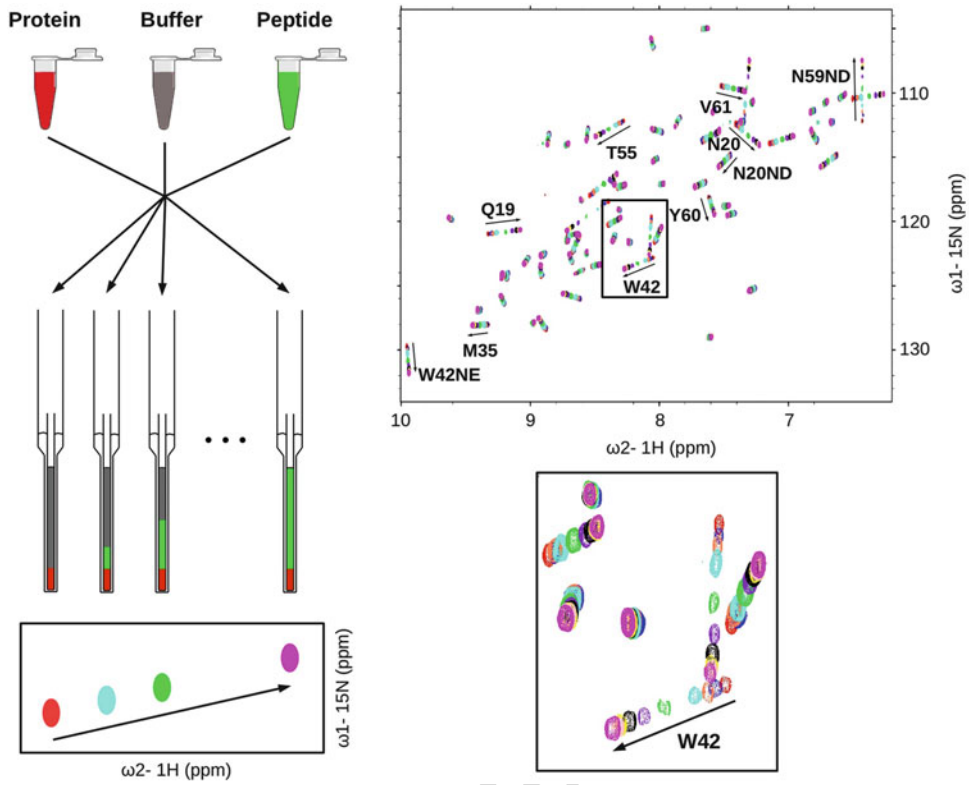

Fig. 3 Preparation of capillary tubes (*left*) for $^{1}H–^{15}N$ HSQC measurements (*right*). The insert shows a close-up on the effect of increasing amounts of peptide on the cross peak corresponding to the backbone amide proton of Tryptophan 42, which is located within the binding site (*see* Fig. 1)

affinity of SH3.3 domain of Vinexin β to a proline rich peptide from the RARγ NTD (*see* **Note 10**).

3. For each sample, record a $^{1}H–^{15}N$ HSQC heteronuclear spectrum with sufficient acquisition time and resolution to allow a precise measurement of nitrogen and proton frequencies.
4. The processed spectra should be superposed in order to identify the $^{1}H–^{15}N$ correlation peaks that are subjected to the largest frequency shifts upon addition of the peptide. Perform a peak-picking on each spectrum in order to compute a composite chemical shift perturbation using:

$$\Delta\delta_{\text{comp}} = \sqrt{(\Delta\delta_{\text{N}})^2 + \left(\frac{\gamma_{\text{H}}}{\gamma_{\text{N}}}\Delta\delta_{\text{H}}\right)^2} \qquad (10)$$

where $\Delta\delta_{\text{N}}$ and $\Delta\delta_{\text{H}}$ are the difference between the nitrogen and proton chemical shifts measured with a given amount of peptide and those measured in absence of peptide. γ_{H} and γ_{N} are the gyromagnetic ratios of the proton and the nitrogen respectively (*see* **Notes 11** and **12**).

t.1 **Table 2**
Composition of samples used for the titration of the C-terminal SH3 domain of human Vinexin β with the P_5VP_5RVYK peptide

t.2 Sample N°	Conc. Peptide stock (μM)	Volume SH3 (μL)	Volume peptide (μL)	Volume buffer (μL)	Conc. SH3 (μM)	Conc. peptide (μM)	Stoichiometric ratio
t.3 1	45	15	0	60	64.4	0	0
t.4 2	45	15	18	42	64.4	10.8	0.17
t.5 3	450	15	3	57	64.4	18	0.28
t.6 4	450	15	6	54	64.4	36	0.56
t.7 5	450	15	15	55	64.4	90	1.40
t.8 6	4,500	15	3	57	64.4	180	2.80
t.9 7	4,500	15	6	54	64.4	360	5.59
t.10 8	4,500	15	12	48	64.4	720	11.18
t.11 9	4,500	15	16	44	64.4	960	14.91
t.12 10	4,500	15	30	30	64.4	1,800	27.95
t.13 11	4,500	15	50	10	64.4	3,000	46.58

3.4 Data Analysis and Error Estimates

The first step of the analysis consists in estimating the number of peptide binding site on the protein surface. (1) a single binding site and one step binding mechanism are characterized by a linear trajectory of the peak in the ^{1}H–^{15}N HSQC series [6, 7, 9]. This should be carefully checked, as the K_d is only defined under these conditions. (2) Further check can be performed by mapping the location of the corresponding amino acids on the protein structure, if both the structure and the HSQC assignment are known (*see* **Note 13**). (3) A last insight is provided by the numerical analysis of chemical shift data. The fitting procedure described below may first be applied using individual ^{1}H–^{15}N correlations first to extract local K_d values. Their convergence to an identical dissociation constant provides a strong indication that these ^{1}H–^{15}N sites monitor the peptide occupancy of the same binding site (*see* **Note 14**).

1. Find the values of K_d and $\Delta\delta_{\text{comp}}^{\max}$ that leads to a minimal value of Eq. 8. This could be performed using least-square fitting procedures available in CcpNmr or other protein NMR software packages. We recommend using Python scripts which offers more flexibility in data analysis and plotting (*see* **Note 15**). Average the Chemical shift changes of Amide groups that belong to the same binding site in order to increase the precision of the binding site occupancy measurement. In case of the Vinexinβ SH3.3 domain, an average chemical shift

perturbation was calculated from 10 ^{1}H–^{15}N correlations corresponding to residues Q19, N20, N20ND, M35, W42, W42NE, T55, N59ND, Y60, and V61 (highlighted in Fig. 3).

2. Estimate the uncertainty on the resulting K_d values. This is done using a Monte Carlo simulation where synthetic datasets are generated and subsequently fitted. These synthetic datasets are generated using a Gaussian distribution of $\Delta\delta_{comp}$ using the values calculated from the first fit as the mean and the root-mean square deviation (the square root of Eq. 8) as the standard deviation. The uncertainties on protein and peptide concentrations are taken into account by generating distributions of peptide and protein total concentrations around the initial values. The width of the distribution is given by the uncertainties on the concentrations (*see* **Note 16**). As concentration values can't be negative, the Log-normal distribution is chosen to generate the distribution of concentration values [10]. The distribution width is then directly given by the relative uncertainties on the measured concentrations (*see* **Notes 17** and **Note 18**).

4 Notes

1. The protocol used to purify the C-terminal SH3.3 domain of human Vinexinβ (REFSEQ: NP 001018003) was a classical two steps purification protocol (Glutathione affinity and gel filtration) that is described in ref. 8. Alternatively, ^{13}C, ^{15}N double-labeled proteins are also suitable for titration experiments. The final buffer was a low salt phosphate buffer with 20 mM sodium phosphate at pH 7.0, 100 mM NaCl.

2. We used a BRUKER Avance III 700 MHz spectrometer equipped with a TCI cryoprobe and a BACS60 sample changer. ^{1}H–^{15}N-HSQC spectra were recorded with 32 scans and 128 data points in the indirect dimension resulting in a total acquisition time of 90 min per sample.

3. Several precautions may be used to prevent, or at least slow down protein degradation. Antiproteases are usually added to the final sample as well as sodium azide (NaN_3) (0.01 % w/v) used as an antibacterial. If the protein sequence contains free cysteines, we usually add reducing agents such as Dithiothreitol (DTT) or TCEP (Tris(2-carboxyethyl)phosphine). In that case, all used buffers should be carefully degassed and oxygen removed from the sample by Helium or Argon bubbling.

4. Protocols used for peptide synthesis and purification lead to the presence of significant amount of trifluoro acetic acid (TFA) salts in dry peptide samples. NMR provides an accurate method

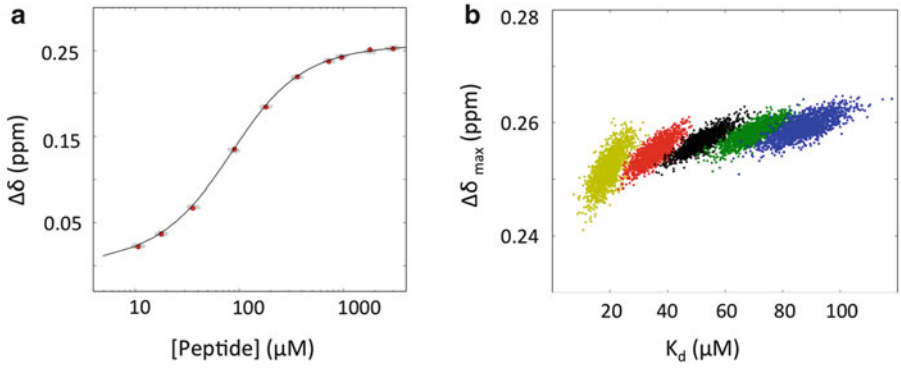

Fig. 4 Least-square fit of the chemical shifts perturbation data measured for the interaction between the P_5VP_5RVYK model peptide and the Vinexinβ SH3.3 domain. (**a**) Semi-log plot of the composite chemical shifts computed from ten residues of SH3.3 as a function of peptide concentrations. Pseudo experimental points generated for the Monte Carlo estimate of the uncertainty on the K_d value are shown in *gray*. These points are distributed according to a gaussian distribution for the Δδ values and according to a log-normal distribution for the peptide and protein concentrations. (**b**) Distribution of the two fitted parameters after the Monte Carlo procedure. The concentration uncertainties were estimated to be 10 % for the SH3.3 protein and between 4 and 5 % for the peptide. The calculations were performed for a peptide stock solution whose concentration was either underestimated by a factor of 0.6 and 0.8 (*yellow* and *red*), or overestimated by 1.2 and 1.4 (*green* and *blue*). The *black points* reflect the effect of pure random noise of the fitting procedure as the concentration of peptide stock solution is considered to be accurate

to check both the efficiency of the desalting procedure and the purity of the final peptide solution by recording ^1H and ^{19}F 1D spectra of the stock peptide solution. Depending on the peptide sequence, we found that the gel filtration desalting method may leave significant amounts of residual trifluoroacetate salts in the final sample. In this case, more efficient protocols should be considered [11].

5. Over or underestimated values of the peptide stock concentration have a dramatic impact on the K_d values resulting from the fit of Eq. 8. This effect can be evaluated by performing Monte Carlo simulations with systematically biased values of ligand concentrations (20 or 40 % above or below the true value, as shown in Fig. 4 and Table 3). The results obtained indicate that a concentration of ligand peptide that is underestimated by 30 % leads to an overestimation of the affinity by a factor of 30 % (The apparent K_d value is 36 μM instead of 52 μM). This large effect is due to the high correlation that exists between the different measurement points since the corresponding protein–peptide mixtures are usually prepared from the same peptide stock solution.
6. A method has been recently proposed to compute the molar absorptivity of a protein or peptide at 205 nm from its amino acid sequence, providing an alternative for quantifying peptides

Table 3 t.1
Average values and standard deviations of dissociation constants (K_d) and chemical shift perturbations ($\Delta\delta_{max}$) values computed from Monte Carlo calculations AU6

	Relative uncertainties (one standard deviation) on peptide concentrations					t.2
	10 %	**20 %**	**30 %**	**40 %**	**50 %**	t.3
K_d (μM)	52.3 ± 5.6	52.0 ± 9.9	52.5 ± 14.6	53.9 ± 19.8	52.3 ± 22.3	t.4
$\Delta\delta_{max}$ (ppm)	0.257 ± 0.002	0.256 ± 0.003	0.256 ± 0.005	0.256 ± 0.006	0.255 ± 0.007	t.5

	Ratio between measured and real peptide concentrations					t.6
	0.6	**0.8**	**1.**	**1.2**	**1.4**	t.7
K_d (μM)	19.6 ± 3.8	35.6 ± 4.2	52.1 ± 5.4	69.8 ± 6.1	87.4 ± 7.3	t.8
$\Delta\delta_{max}$ (ppm)	0.252 ± 0.003	0.255 ± 0.002	0.257 ± 0.002	0.258 ± 0.002	0.259 ± 0.002	t.9

Experimental chemical shifts were obtained from the interaction of the P_5VP_5RVYK peptide with the Vinexinβ SH3.3 domain. The uncertainty of the SH3.3 protein concentration was estimated to be 10 %. The fitted values are reported for different uncertainties of the peptide concentrations (*upper panel*) or for a systematic error on peptide stock solution (*lower panel*). t.10

lacking tryptophan or tyrosine residues [12]. Combining this measurement with the quantitative evaluation of peptide concentration by NMR provides an interesting way to get robust estimates of concentrations. Other methods have been proposed for protein concentrations measurements by NMR, such as PULCON for instance [13].

7. In order to increase the precision of this OD measurement, we usually perform several $OD_{280\ nm}$ measurements with targeted absorption values of 0.8, 0.4, 0.2, and 0.1. The linear regression of this series of measurements is used to provide an estimation of the uncertainty on the Tryptophan stock solution concentration.
8. The Signal-to-Noise ratio (S/N) in NMR may be written as:

$$S/N \propto \frac{M_0 B_1}{\sqrt{P_s(T_a + T_s) + P_c(T_a + T_c)}} \qquad (11)$$

where M_0 is the spin magnetization, B_1 the radio-frequency (RF) field intensity applied to the sample, and P_c and P_s are the RF power absorbed by the coil and by the sample, respectively. T_c and T_s are the temperature of the coil and the sample, respectively, while T_a is the noise temperature of the preamplifier [14–16]. Recent progress in NMR probe development, most notably the development of cryogenic probes, improved the S/N by lowering T_c and T_a down to 10–25 K and by reducing P_c by optimizing the coil quality factor (*see* ref. 16).

There remains room for S/N optimization on the P_s term, which is mostly dependent on the sample itself because of dielectric losses. It is known that the RF power dissipated in the sample depends on the dielectric constant of the medium which is very much dependent on the type of solvent and on the ionic strength when working in H_2O. Thus, the P_s term depends on the distribution of the electric field within the sample geometry and on the strength of the RF irradiation (expressed as its angular frequency ω_1) with:

$$P_S \propto \omega_1^2 \tag{12}$$

Because of this dependency, P_s losses become more prominent with increasing fields. On a given probe, reducing the internal diameter of the NMR tube with a capillary system has two opposite effects on the overall sensitivity of the measurement. First, reducing the sample volume at a given concentration results in a loss of signal due to a proportional reduction of sample quantity. However, the power dissipated within the sample P_s is also reduced and so is the noise, leading to a potential improvement of the S/N. The balance between these two effects strongly depends on the nature of the sample itself, and the amount of the overall effect is not directly predictable. Finally, it should be mentioned that the use of capillary tubes centers the sample in the inner volume of the coil where the electric field is minimum and the impact on P_s and thus on the noise is maximum. This effect has been studied [17] and it was shown that in high salt conditions it is actually beneficial in terms of S/N to reduce the NMR tube diameter while keeping all concentrations constant.

9. This gain results from several factors. First, the signal noise arising from RF losses in the sample itself is minimized in small diameter tubes due to a lower value of P_s, the RF power dissipated within the sample (*see* **Note 8**). This effect will be of increasing importance if high salt concentrations are required for the protein buffer and if a cryogenically cooled probe is used. A second source of sensitivity gain originates from a more optimal use of the sample volume as only about 30 % of the sample volume is outside the RF coil. On 5 mm tubes, susceptibility matched NMR tubes or plugs (Shigemi tubes) are usually used to compensate this effect, allowing doubling the relative sensitivity. Though the handling of these systems is cumbersome, the susceptibility matched approach can also be applied on capillary tubes, with a potential further 43 % gain in relative sensitivity. Finally, the use of an external lock implies that there is no need to add deuterium into the sample itself which otherwise leads to an additional loss of signal due to deuterium exchange of the amide protons. Notably, the

capillary sample lacking 9 % D2O enables another 21 % of gain in relative sensitivity.

10. In our example, the concentration of the protein is constant while the peptide concentration varies. It has been shown that an optimal sampling is achieved when both the protein and peptide concentrations are varied together [18].
11. Peak picking is usually performed using the software packages dedicated to protein NMR spectra analysis such as SPARKY (http://www.cgl.ucsf.edu/home/sparky), CcpNmr Analysis (http://www.ccpn.ac.uk) or CARA (http://cara.nmr.ch). Peak tracking can be performed with algorithms such as described in [19] for instance.
12. The ratio γ_H/γ_N is a weighting factor that compensates the difference of chemical shift ranges between proton and nitrogen frequencies. Its precise value is of little importance and there are also other weighting factors described in the literature.
13. The resonance assignment of a variety of proteins can be obtained from the Biological Magnetic Resonance Data Base (BMRB) at http://www.bmrb.wisc.edu/.
14. The knowledge of the resonance assignments is not required to identify two binding sites if their affinity are different and if this difference could be resolved by NMR titration experiments as shown in [6].
15. The set of Python script used to analyze the interaction between the Vinexinβ SH3.3 domain and the P_5VP_5RVYK RARγ model peptide is available at http://zenodo.org (doi: 10.5281/zenodo.11663).
16. The propagation of uncertainties of volume measurements follows the general law:

$$u^2(y) = \sum_{i=1}^{N} \left(\frac{\partial f}{\partial x_i}\right)^2 u^2(x_i) + 2\sum_{i=1}^{N-1}\sum_{j=i+1}^{N} \frac{\partial f}{\partial x_i}\frac{\partial f}{\partial x_j}\mathrm{cov}(x_i, x_j) \tag{13}$$

where $u(y)$ is the uncertainty on the concentration that depends on several variables ($y = f(x_i)$) depending on the specific scheme that is used for sample preparation. The covariance ($y = f(x_i)$) was set to 1 for volumes if the same pipette was used twice, and for concentrations when the same solution was used. The calculation of uncertainty propagation used for the Vinexinβ work is available at the following address: http://zenodo.org (doi: 10.5281/zenodo.11663).

17. Two main types of uncertainties have to be distinguished: an erroneous estimation of the peptide stock solution will lead to a

t.1 **Table 4**
Comparison of the uncertainties on ligand concentrations for sequential or parallel titration experiments

t.2			Absolute (μM) and relative ligand concentration uncertainties	
t.3	Sample number	Peptide concentration (μM)	Sequential titration scheme	Parallel titration scheme
t.4	0	0.0		
t.5	1	10.8	4.8 % (0.52)	4.9 % (0.53)
t.6	2	18.0	3.7 % (0.66)	4.9 % (0.89)
t.7	3	36.0	4.1 % (1.49)	4.8 % (1.74)
t.8	4	90.0	5.4 % (4.84)	4.8 % (4.28)
t.9	5	180.0	5.8 % (10.5)	4.8 % (8.66)
t.10	6	360.0	6.7 % (24.3)	4.7 % (16.9)
t.11	7	720.0	7.4 % (53.5)	4.6 % (33.3)
t.12	8	960.0	6.4 % (61.9)	4.6 % (44.3)
t.13	9	1800.0	7.0 % (126.3)	4.6 % (82.7)
t.14	10	3000.0	5.1 % (152.7)	4.5 % (135.4)
t.15		Max uncertainty:	7.4 %	4.9 %

systematic bias in the resulting K_d values, while pipetting errors will introduce random noise on the measurements. We have simulated both effects and the resulting uncertainties on fitted parameters are shown in Table 3. While a random noise of 20 % on the peptide concentration leads to a resulting relative uncertainty of 20 % on the K_d value, a 20 % underestimation of the peptide concentration leads to overestimation of the affinity by more than 30 % (36 μM instead of 52 μM). This emphasizes the importance of having the most accurate peptide concentration values before undertaking affinity measurements by NMR or by any other methods.

18. In order to provide a quantitative estimation of these effects, we performed formal calculations to compute the uncertainties on the protein and peptide concentrations for each point of the titration that arise from the uncertainties of volume measurements. These later values were taken from the specifications provided by the pipette manufacturer (Gilson Inc.). The resulting absolute and relative uncertainties on the ligand concentrations together with their impact on the resulting K_d are reported in Table 4. The parallel titration protocol leads to

maximal relative error on ligand concentrations of 4.9 %, a value that is lower than the one obtained (7.4 %) if the experiment would have been performed using a regular sequential addition of ligand to the same tube. It is worth noting that this calculation is probably underestimating the uncertainty associated with the sequential titration protocol as the multiple manipulations of the same tube will lead to unavoidable losses of sample volume, in particular when susceptibility matching tubes are used.

Acknowledgments

This work was supported by the ANR program VINRAR ANR-09-BLAN-0297, the Institut National du Cancer [grant number INCa-PL09-194], the Ligue Regional contre le cancer and by the French Infrastructure for Integrated Structural Biology (FRISBI) ANR-10-INSB-05-01, as part of the European Strategy Forum on Research Infrastructures (ESFRI) and through national members agreements. The authors thank Claude Ling (IGBMC) for technical support, the chemical peptide synthesis service at IGBMC and Yves Nominé for critical reading of the manuscript.

References

1. Kieffer B, Homans S, Jahnke W (2011) Nuclear magnetic resonance of ligand binding to proteins. In: Podjarni A, Dejaegere A, Kieffer B (eds) Biophysical approaches determining ligand binding to biomolecular targets. RSC, Cambridge, UK, pp 15–55
2. Fielding L (2007) NMR methods for the determination of protein–ligand dissociation constants. Prog Nucl Magn Reson Spectrosc 51:219–242
3. Dalvit C (2009) NMR methods in fragment screening: theory and a comparison with other biophysical techniques. Drug Discov Today 14:1051–1057
4. Pellecchia M, Bertini I, Cowburn D, Dalvit C, Giralt E, Jahnke W, James TL, Homans SW, Kessler H, Luchinat C, Meyer B, Oschkinat H, Peng J, Schwalbe H, Siegal G (2008) Perspectives on NMR in drug discovery: a technique comes of age. Nat Rev Drug Discov 7:738–745
5. Sprangers R, Kay LE (2007) Quantitative dynamics and binding studies of the 20S proteasome by NMR. Nature 445:618–622
6. Quinternet M, Starck JP, Delsuc MA, Kieffer B (2012) Unraveling complex small-molecule binding mechanisms by using simple NMR spectroscopy. Chem Eur J 18:3969–3974
7. Bourry D, Sinnaeve D, Gheysen K, Fritzinger B, Vandenborre G, Van Damme EJ, Wieruszeski JM, Lippens G, Ampe C, Martins JC (2011) Intermolecular interaction studies using small volumes. Magn Reson Chem 49:9–15
8. Lalevee S, Bour G, Quinternet M, Samarut E, Kessler P, Vitorino M, Bruck N, Delsuc MA, Vonesch JL, Kieffer B, Rochette-Egly C (2010) Vinexinß, an atypical "sensor" of retinoic acid receptor gamma signaling: union and sequestration, separation, and phosphorylation. FASEB J 24:4523–4534
9. Williamson MP (2013) Using chemical shift perturbation to characterise ligand binding. Prog Nucl Magn Reson Spectrosc 73:1–16
10. Limpert E, Stahel WA, Abbt M (2001) Log-normal distributions across sciences: keys and clues. Bioscience 51:341–352
11. Roux S, Zekri E, Rousseau B, Paternostre M, Cintrat JC, Fay N (2008) Elimination and exchange of trifluoroacetate counter-ion from cationic peptides: a critical evaluation of different approaches. J Pept Sci 14:354–359

12. Anthis NJ, Clore GM (2013) Sequence-specific determination of protein and peptide concentrations by absorbance at 205 nm. Protein Sci 22:851–858
13. Wider G, Dreier L (2006) Measuring protein concentrations by NMR spectroscopy. J Am Chem Soc 128:2571–2576
14. Hoult DI, Lauterbur PC (1979) The sensitivity of the zeugmatographic experiment involving human samples. J Magn Reson 34:425–433
15. Hoult DI (1996) Sensitivity of the NMR experiment. In: Grant DM (ed) Encyclopaedia of nuclear magnetic resonance. Wiley, New York, NY
16. de Swiet TM (2005) Optimal electric fields for different sample shapes in high resolution NMR spectroscopy. J Magn Reson 174:331–334
17. Voehler MW, Collier G, Young JK, Stone MP, Germann MW (2006) Performance of cryogenic probes as a function of ionic strength and sample tube geometry. J Magn Reson 183:102–109
18. Markin CJ, Spyracopoulos L (2012) Increased precision for analysis of protein-ligand dissociation constants determined from chemical shift titrations. J Biomol NMR 53:125–138
19. Ravel P, Kister G, Malliavin TE, Delsuc MA (2007) A general algorithm for peak-tracking in multi-dimensional NMR experiments. J Biomol NMR 37:265–275
20. Kovrigin EL (2012) NMR line shapes and multi-state binding equilibria. J Biomol NMR 53:257–270

Author Queries

Chapter No.: 22 317550_3_En

Query Refs.	Details Required	Author's response
AU1	Please check whether the affiliations of the authors are presented appropriately.	
AU2	Please check whether the edited value in the sentence "1.7 mm outer-diameter capillary system. . ." is appropriate.	
AU3	Please check whether the values (bold, italic) are presented appropriately throughout the chapter (both in equations and text).	
AU4	Please provide the significance for "bold emphasis" given in the Table 1.	
AU5	The list starting with "Find the values of Kd and. . ." has been renumbered. Please check.	
AU6	Please check whether the footer presented in Table 3 is appropriate.	
AU7	Note that reference [20] (original [8]) is not cited in text. Please cite the reference in text or delete it from the list.	
AU8	Note that refs. 2b, 6b, and 11b has been renumbered and cited sequentially in text. Please check whether the cross references are appropriate.	
AU9	Please check whether the article title in ref. [8], is presented appropriately.	